AIP | Review of Scientific Instruments

VINETA II: A linear magnetic reconnection experiment

H. Bohlin, A. Von Stechow, K. Rahbarnia, O. Grulke, and T. Klinger

Citation: Review of Scientific Instruments **85**, 023501 (2014); doi: 10.1063/1.4861359
View online: http://dx.doi.org/10.1063/1.4861359
View Table of Contents: http://scitation.aip.org/content/aip/journal/rsi/85/2?ver=pdfcov
Published by the AIP Publishing

VINETA II: A linear magnetic reconnection experiment

H. Bohlin,[1,a)] A. Von Stechow,[1] K. Rahbarnia,[1] O. Grulke,[1] and T. Klinger[1,2]
[1]*Max-Planck-Institute for Plasma Physics, EURATOM Association, Wendelsteinstr. 1, 17491 Greifswald, Germany*
[2]*Ernst-Moritz-Arndt University, Domstr. 11, 17489 Greifswald, Germany*

(Received 18 November 2013; accepted 22 December 2013; published online 4 February 2014)

A linear experiment dedicated to the study of driven magnetic reconnection is presented. The new device (VINETA II) is suitable for investigating both collisional and near collisionless reconnection. Reconnection is achieved by externally driving magnetic field lines towards an X-point, inducing a current in the background plasma which consequently modifies the magnetic field topology. Owing to the open field line configuration of the experiment, the current is limited by the axial sheath boundary conditions. A plasma gun is used as an additional electron source in order to counterbalance the charge separation effects and supply the required current. Two drive methods are used in the device. First, an oscillating current through two parallel conductors drive the reconnection. Second, a stationary X-point topology is formed by the parallel conductors, and the drive is achieved by an oscillating current through a third conductor. In the first setup, the magnetic field of the axial plasma current dominates the field topology near the X-point throughout most of the drive. The second setup allows for the amplitude of the plasma current as well as the motion of the flux to be set independently of the X-point topology of the parallel conductors. © *2014 AIP Publishing LLC*. [http://dx.doi.org/10.1063/1.4861359]

I. INTRODUCTION

Magnetic reconnection is a topological rearrangement of magnetic fields resulting in a conversion of magnetic energy into kinetic and thermal energy.[1–3] This process takes place in the current sheet formed at the boundary between opposed magnetic fields and is thought to play an important role in space phenomena, such as solar flares[4] and at Earth's magnetosphere,[5] as well as in fusion experiments.[6,7] Despite intense research on the topic over the last decades and a vast quantity of information obtained through space observations,[8,9] numerical simulations,[10,11] and experiments,[12–19] the underlying processes of magnetic reconnection are still not fully understood. For plasmas with high resistivity and small length scales, simple magnetohydrodynamic (MHD) models give an adequate description of reconnection.[4,20,21] However, these models are insufficient when describing reconnection in nearly collisionless plasmas and it has been found that the reconnection proceeds much faster than predicted in these cases.[1] It is widely believed that fast collisionless reconnection is facilitated through two-fluid Hall processes[22] as well as through anomalous resistivity due to fluctuations in the current sheet.[23] The relative importance of the two processes is however under debate.[2]

One of the major unresolved issues of reconnection is exactly how the magnetic energy is converted to kinetic energy of the electrons and ions, a process which has, for example, been indirectly observed through X-ray images of solar flares.[24] The description of reconnection is often simplified by using two-dimensional geometry, however, a magnetic field component perpendicular to the reconnection field (guide field) has been found to play an important role in the dynamics of reconnection.[25,26] Both the reconnection rate[12] as well as the shape of the current sheet[27,28] has been observed to be affected by the guide field component. Other unresolved issues include how global boundary conditions influence reconnection and the cause for impulsive reconnection.[1–3]

The observation of reconnection in space and fusion plasmas is often hampered by technical limitations and harsh environments. Dedicated experiments provide a wide range of plasma parameters and enable a controllable environment which allows for a detailed study of the mechanisms involved in reconnection. There are a number of past and present day devices devoted to the study of magnetic reconnection, with one of the earliest experiments carried out by Stenzel and Gekelmann[28] on a linear device at UCLA.[12] Other major experiments include TS-3/4 at the University of Tokyo,[13] the Magnetic Reconnection Experiment (MRX) at the Princeton Plasma Physics Lab,[14] the Versatile Toroidal Facility (VTF) at the Massachusetts Institute of Technology,[15] 3D-CS at the General Physics Institute Russian Academy of Sciences,[16] the Swarthmore Spheromak Experiment (SSX) at Swarthmore College,[17] the Reconnection Scaling Experiment (RSX) at the Los Alamos National Laboratory,[18] and the Rotating Wall Machine (RWM) at the University of Wisconsin.[19] For an overview of reconnection devices and the progress made through experiments and numerical simulations in the field of reconnection, comprehensive reviews were published by Yamada *et al.*[2] and Zweibel and Yamada.[29]

The study of the detailed physical processes involved in reconnection necessitates an experimental device with plasma parameters which allow for the study of kinetic effects as well as the formation of current sheets large enough to be spatially resolved with the available diagnostics. The new linear device VINETA II has been designed for the study of driven magnetic reconnection. The experiment utilizes two parallel

a)hannes.bohlin@ipp.mpg.de

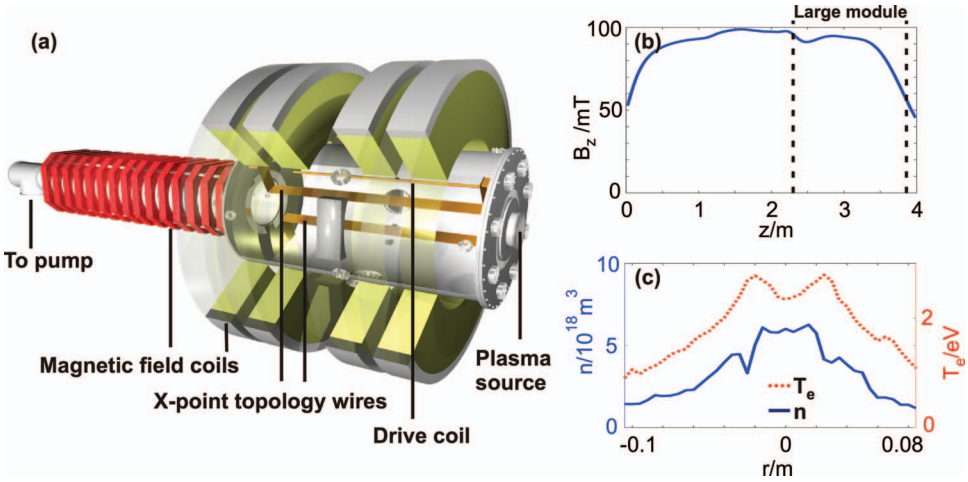

FIG. 1. (a) Schematic drawing of the VINETA II device. (b) Guide field along the device axis at the center. The dashed lines indicate the large module. (c) Radial profiles of density (solid line) and electron temperature (dotted line).

conductors for creating an X-point topology. The drive of the field lines is achieved by an oscillating current through either the two conductors or through an additional third coil. The main aims and issues to be addressed are the following: 1. Transition from resistive to collisionless reconnection. 2. Reconnection in partially ionized plasmas. 3. The influence of global boundary conditions. 4. Reconnection with a significant guide field component and three-dimensional reconnection. 5. Particle kinetics in the current sheet. 6. Study of electromagnetic fluctuations in the current sheet and coupling of externally driven fluctuations to the reconnection event.

The paper is organized as follows: In Sec. II A, the experimental device VINETA II is presented. In Sec. II B, two methods for driving the reconnection are described. In addition, limitations given by the open field line configuration are discussed and the need for a plasma gun as an electron source is justified. In Sec. II C, the achievable reconnection regimes are described and the major diagnostics used in the experiment are outlined in Sec. II D. In Sec. III, initial results for the two driving methods are presented. Section IV gives a summary and conclusions.

II. EXPERIMENTAL SETUP

A. VINETA II

A schematics of VINETA II, the new experimental setup, is shown in Figure 1(a). The device consists of a stainless steel vacuum chamber with a diameter of 1 m and a length of 1.6 m, in combination with two smaller modules.[30] The two sets of magnetic field coils generate a homogeneous axial guide field of $B \leq 100$ mT along the device. The calculated guide field at the device axis is shown in Figure 1(b). There is a gradient of the magnetic field at the end of the large module on the plasma source side. If needed, the fringing field effect of the guide field can be eliminated by rearranging the experiment to have a small module on each side of the large one. Three conductors within the vacuum chamber create the reconnection magnetic field and drive the reconnection. A detailed description of the reconnection drive is given in Sec. II B. The two flat conductors have a width of 10 cm and are positioned close to the plasma at $r = 15$ cm. The calculated magnetic field and X-point field line topology produced by the two parallel conductors are shown in Figure 2(a). It is clearly possible to establish a closed field line configuration which largely avoids parallel plasma transport to the walls along the reconnecting field lines. A third smaller cylindrical conductor is placed at a 90° angle to the flat conductors at a radial position of 0.4 m.

A background plasma is generated using either a half-turn double helicon antenna[31] or a spiral antenna.[32] This allows for plasma densities spanning over $n = 10^{16} - 10^{19}$ m^3 and electron temperatures of up to 6 eV. The radial profiles of the electron temperature and density for a helicon discharge are shown in Figure 1(c). The dip in temperature and flattening of the density profile at the center is owing to the plasma gun being placed at the axis.

B. Reconnection drive

Reconnection in VINETA II is achieved by externally driving the magnetic field lines towards the X-point, thereby inducing a current in the background plasma which consequently modifies the magnetic field topology. The oscillating current for the drive is produced via a resonant LC circuit. The inductance of the reconnection wire in combination with a variable capacitance allows for a frequency range of the drive of between 60 and 100 kHz. The frequency dependence of the maximum absolute value of the current through the conductors is shown in Figure 2(b). Due to the increasing impedance, the current amplitude decreases with increasing drive frequency. The choice of the frequency is based on a compromise between the time resolution of the available diagnostics and making the resistive layer width small enough for kinetic effects to be important.[1] The resistive layer width is given by[1]

$$\Delta_{res} = \sqrt{\frac{2\eta\tau_{drive}}{\mu_0}}. \quad (1)$$

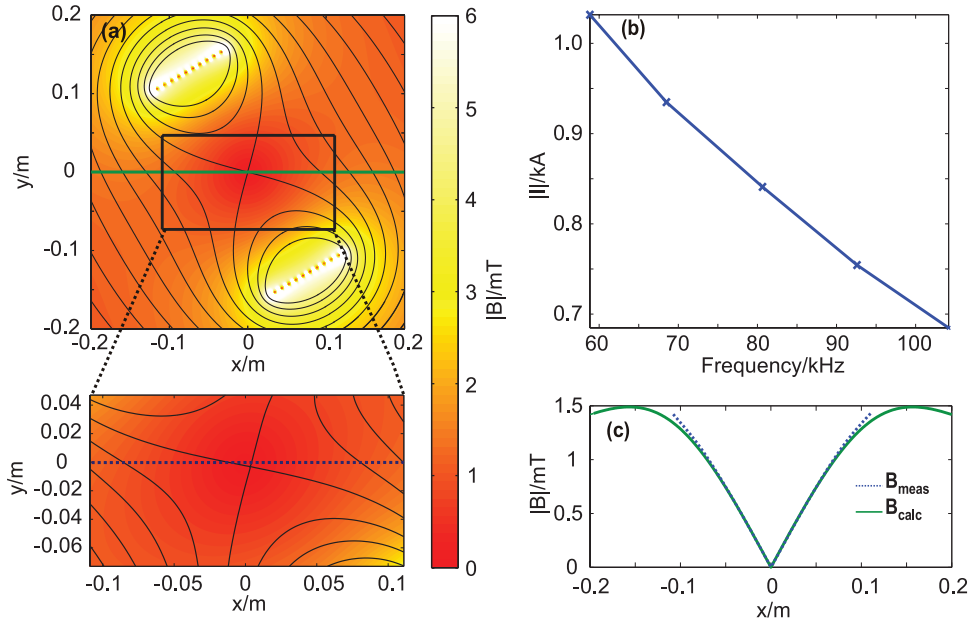

FIG. 2. (a) Frequency dependence of reconnection drive current. (b) Azimuthal cut of calculated absolute magnetic field for a current of 1 kA/m, with contours of constant vector potential representing magnetic field lines. The black box indicates the measurement region and the blow-up shows a measurement with induction coils in vacuum. (c) One-dimensional cuts of the measured (dotted) and calculated (solid) magnetic field.

Here, τ_{drive} is the timescale of the reconnection (set by the reconnection drive) and η is the resistivity. For the study of kinetic effects, Δ_{res} must be smaller than the kinetic spatial plasma scales,[1] i.e., the collisionless skin depth δ and the ion sound gyroradius ρ_s, defined as

$$\delta = \frac{c}{\omega_{pe}} \quad , \quad \rho_s = \frac{c_s}{\omega_{ci}} \, . \tag{2}$$

Here, c denotes the speed of light, ω_{pe} the electron plasma frequency, c_s the ion sound speed, and ω_{ci} the ion gyro frequency.

Due to the open field line configuration of the experiment, the plasma current generated in response to the drive is not free to flow, but is limited by the axial sheath boundary conditions. This results in the build-up of an electrostatic electric field along the guide field, which counterbalances the inductive electric field to provide ambipolarity of the fluxes to the walls. Assuming a collisionless sheath boundary condition and using the Bohm sheath criterion, the Debye flux yields a current density of[33]

$$j_D = nec_s \left(1 - e^{\Lambda - \Phi/T_e}\right) \, . \tag{3}$$

Here, c_s is the ion sound speed and $\Lambda = \ln\sqrt{M_i/2\pi m_e}$ with M_i the ion mass and m_e the electron mass. Taking the central temperature and density values shown in Figure 1(c) and making the assumption that Φ is approximately 2–3 times the electron temperature, this sets an upper limit of the current density at the X-point of $J_D \approx 2$ kA/m^2. In comparison, assuming Spitzer resistivity, an inductive electric field generated by the reconnection drive of $E_{ind} \approx 150$ V/m requires a current density of $j \approx 500$ kA/m^2. Thus, an additional electron source is needed to counterbalance the charge separation effect and to provide the current in response to the inductive field. In VINETA II, this is achieved using a plasma gun, which produces electrons through an arc discharge.[34]

Two approaches are utilized for driving the reconnection. The first, called setup A, drives the oscillating current through the two parallel conductors, thus compressing the magnetic field towards the X-point. For the second approach, called setup B, a nearly constant current of $I_c \leq 1$ kA, produced by a pulse forming network (PFN),[35] through the conductor pair produces a stationary X-point magnetic field topology as shown in Figure 2(a). The oscillating current produced by the drive circuit through a third conductor generates an inductive field, E_{ind} which drives the magnetic field towards the X-point by $\mathbf{E} \times \mathbf{B}$ drift. For both setups, the drive of the reconnection is independent of the plasma generation, i.e., plasma parameters such as density and temperature can be varied without affecting the drive. For setup B, the inductive field can also be set independently of the amplitude of the in-plane magnetic field.

C. Reconnection regimes

Based on the commonly accepted models,[1] magnetic reconnection in space and laboratory devices is subdivided in different regimes such as collisional/collisionless, single/multiple X-line reconnection, and hybrid branches.[2,36] The typical plasma and reconnection parameters for two operation regimes are given in Table I. The operation regime of typical Argon discharges in VINETA II is spanned by the dimensionless Lundquist number S

$$S = \frac{\mu_0 L_{CS} v_A}{\eta_{Sp}}. \tag{4}$$

as a function of the effective plasma size λ

$$\lambda = \frac{L}{\rho_s} \, . \tag{5}$$

TABLE I. Typical plasma and reconnection parameters for two operation regimes.

		High density	Low density
Plasma density	n	10^{19} m^{-3}	10^{16} m^{-3}
Electron temperature	T_e	2 eV	6 eV
Magnetic guide field	B_{guide}	100 mT	5 mT
Ion temperature	T_i	0.2 eV	0.2 eV
Reconnection field	B_{rec}	<5 mT	<5 mT
Lundquist number	S	4	450
Drive time	τ_{drive}	10 μs	10 μs
Diffusion time	τ_{diff}	10 μs	30 μs
Resistive layer width	Δ_{res}	7 cm	4 cm
Collisionless skin depth	δ	2 mm	5 cm
Ion sound gyroradius	ρ_s	1 cm	16 cm

Here, η_{Sp} is the Spitzer resistivity and $v_A = B_{rec}/\sqrt{\mu_0 n m_i}$ is the Alfvén speed based on the in-plane reconnection magnetic field component B_{rec}. $L_{CS} = \varepsilon L$ is the length of the current sheet for the plasma size L, where ϵ is typically chosen between[36] $0 \le \epsilon \le 0.5$. Finally, $\rho_s = \sqrt{(T_i + T_e)m_i}/(q_i B_{total})$ is the ion sound gyro radius with B_{tot} being the total magnetic field including both reconnection and guide field components. The broad range of plasma parameters achievable in VINETA II allows for the investigation of both single X-line collisional and collisionless reconnection as shown in Figure 3. The two regimes are divided by a dashed line which is given by $S = \lambda^2/4$. Also indicated in the figure are the changes (increase/decrease) in quantities such as temperature, density, and magnetic field required to transition between the collisional and collisionless branch.

D. Diagnostics

In order to study reconnection it is essential to obtain a detailed description of the electromagnetic fields and currents that, along with the evolution of plasma parameters such as temperature and density, characterize the system. The plasma parameters are obtained using Langmuir probe measurements and the magnetic reconnection field is measured using induction coils[37,38] that are scanned on a shot-to-shot basis through the entire poloidal plasma cross section using a high precision positioning system. This allows for the determination of the well reproducible spatiotemporal evolution of the magnetic field. The magnitude of the field in vacuum as measured with this setup is shown in the blow-up in Figure 2(a). A comparison between the measured and the calculated magnetic field (Figure 2(c)) shows good agreement. The measurements of the magnetic field enables the determination of the time-evolution of the magnetic field lines, which are represented by contours of constant vector potential. Assuming the frozen-in flux condition this also yields the motion of the plasma.[1] The induced axial electric field can be calculated from the probe measurement using $\mathbf{E} = -\partial \mathbf{A}/\partial t$, where $\mathbf{A}$ is the vector potential. The maximum induced electric field is shown in Figures 4(a) and 4(b) for setup A and 4(c) and 4(d) for setup B. The solid line represents a one-dimensional cut through the center in direction towards the parallel conductors and the dotted line a cut perpendicular to the solid line. For setup A, the inductive field has a saddle point at the X-point, with increasing amplitude towards the conductors and decreasing towards zero at the wall of the vacuum chamber. For setup B, the inductive field increases towards the third conductor.

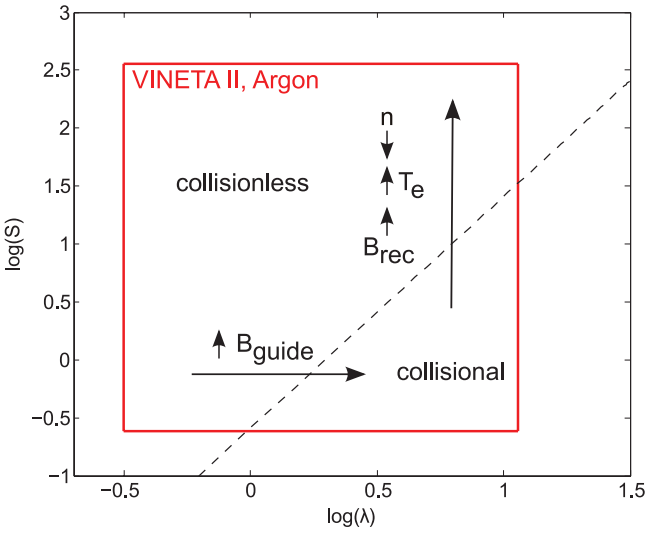

FIG. 3. VINETA II operation regime for Argon. Indicated are the changes for specific quantities to switch between the collisional and collisionless branch divided by the dashed line, which is given by $S = \lambda^2/4$.

III. EXPERIMENTAL RESULTS

First results for the two methods of driving magnetic reconnection in VINETA II are presented subsequently. The experiments are carried out with a relatively strong guide field of 30 mT for setup A and 6 mT for setup B. This gives a ratio of the in-plane to guide magnetic field of, $B_{guide}/B_{rec} \approx 21$ for setup A and $B_{guide}/B_{rec} \approx 6$ for setup B. B_{rec} is taken as the maximum of the in-plane reconnecting field at a position well outside the current sheet (5 cm radially towards the parallel conductors). The absolute magnetic field and current density measurements for reconnection with setup A and B are given in Figures 5 and 6, respectively. Figure 5(a) shows the oscillating current through the two conductors (solid line) and the current extracted from the gun (dashed-dotted line) via the inducted electric field. The extracted current is obtained by spatial integration of the two-dimensional current density. The time-derivative of the drive current is taken as an approximation of the inductive field (dotted line in Figure 5(a)). An initially high electric field is induced as the drive turns on and then follows the current with a $-\pi/2$ phase shift. The maximum inductive field at the center was approximately 150 V/m for this measurement. A small bump in the electric field can be seen as the current through the conductors changes direction, which is related to the switching of the insulated-gate bipolar transistors (IGBT) of the reconnection drive circuit. The current from the gun has an initial peak then decreases within a few microseconds to a small, relatively constant current of a few ampere. This current is most likely due to an electrostatic field in the system. As the reconnection drive sets in, the

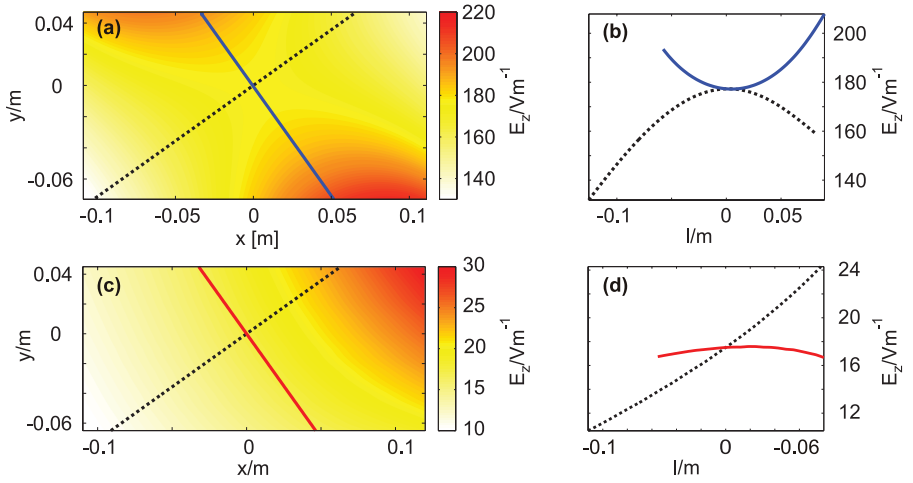

FIG. 4. (a) Amplitude of the axial inductive electric field, E_z, in the azimuthal plane for setup A. (b) One-dimensional cuts through the center in direction towards the conductors (solid line) and perpendicular to the conductors as indicated in (a). (c) and (d) are the same as for (a) and (b) but for setup B.

inductive field initially acts to inhibit this background current, and a current is only inductively extracted from the gun when the inductive field becomes positive i.e., pointing towards the gun. Comparing the inductive field and the extracted current it is clear that the latter does not follow the former perfectly in time. The current starts to flow as soon as the inductive field points in the right direction but does not reach its maximum of 65 A until 0.5 μs after the inductive field does and a current continues to flow 3 μs after the inductive field has changed direction. As with the background current, it is not clear what the cause of this discrepancy is, but one possible explanation could be that the inductance of the gun

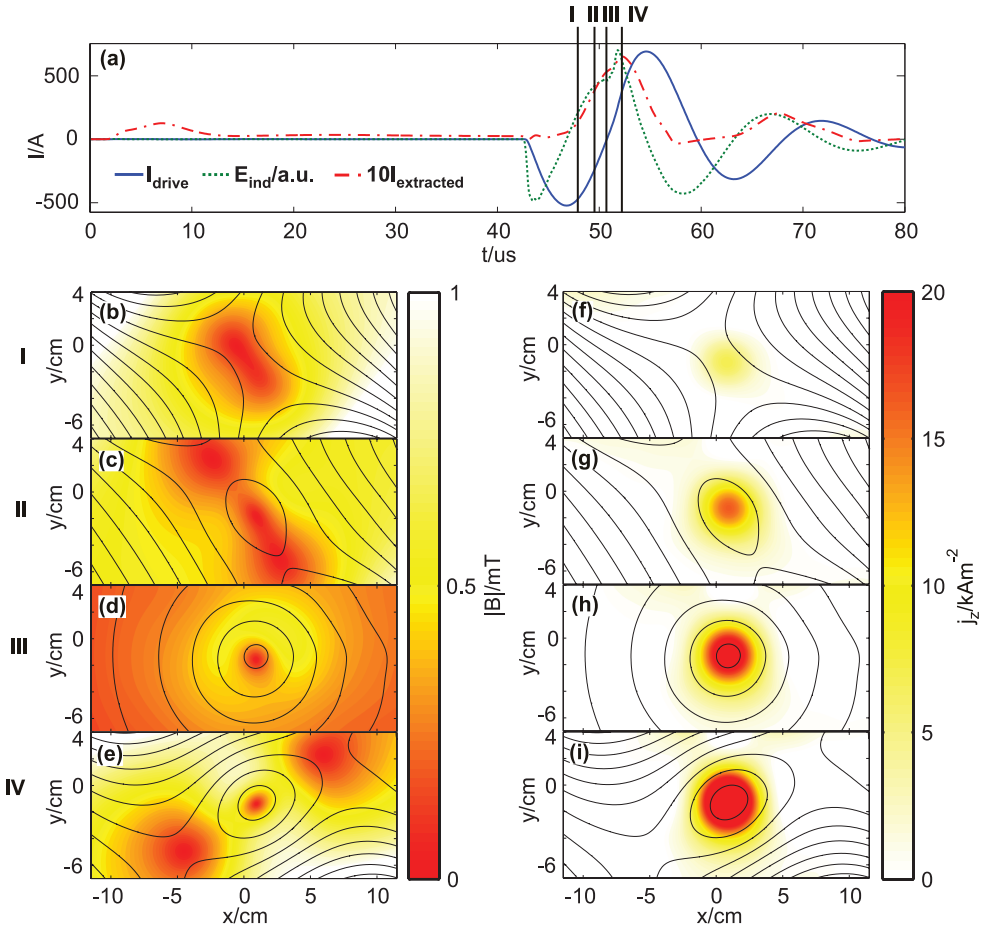

FIG. 5. Setup A. (a) Current traces of reconnection drive (solid line) and extracted current from gun (dashed-dotted line), as well as the time-derivative of the reconnection drive current as an approximation of the inductive field (dotted line). Indicated are four time points, I–IV, for which the absolute magnetic field (b)–(e) and current density (f)–(i) are plotted. Superimposed are contours of constant vector potential which represent magnetic field lines.

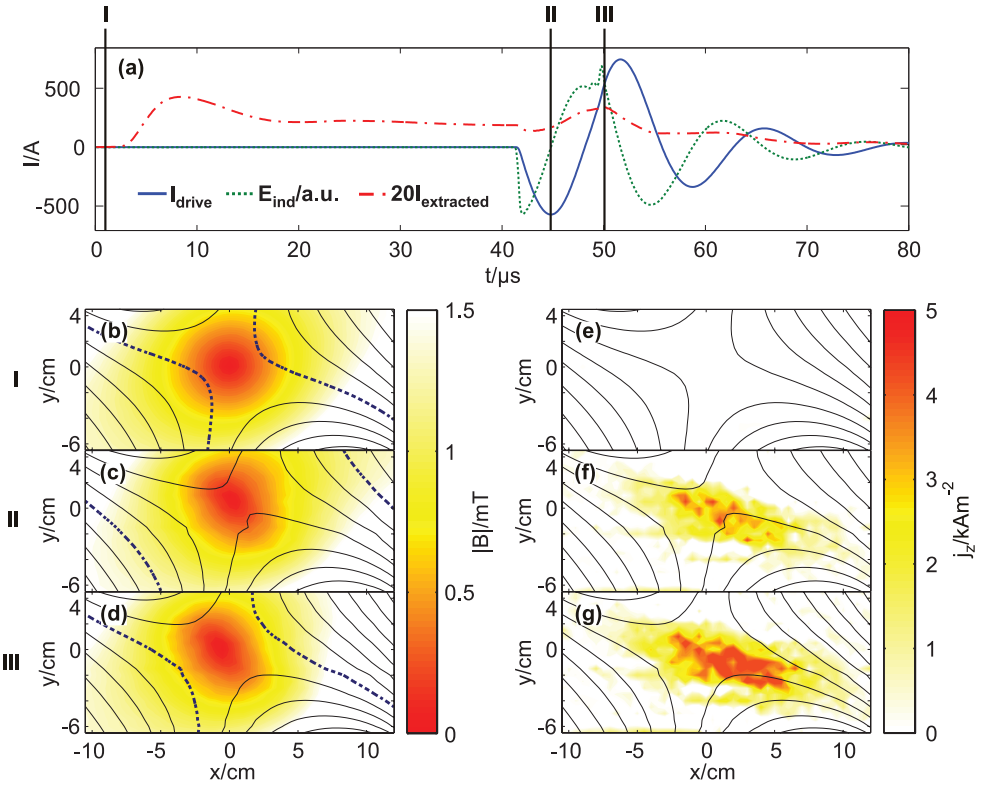

FIG. 6. Setup B. (a) Current traces of reconnection drive (solid line) and extracted current from gun (dashed-dotted line), as well as the time-derivative of the reconnection drive current as an approximation of the inductive field (dotted line). I–III indicate three time points for which the two-dimensional absolute magnetic field and current density has been plotted ((b)–(d) and (e)–(g), respectively).

setup and the plasma acts to inhibit the rise/fall time of the current.

The absolute magnetic field and current density at four time instants (indicated by I–IV in 5(a)) are shown in 5(b)–5(e) and 5(f)–5(i), respectively. Field lines are given by the contours of constant vector potential. The contour levels are plotted for the same values for all time points. Depending on whether the current through the conductors is rising or falling, the field lines are either pushed away from the conductors (IV) or pulled towards them (I and II). When the reconnecting magnetic field is high, but the gun current still relatively low, a neutral sheet is formed (I). However, as the extracted current increases, it becomes the dominant contribution to the in-plane magnetic field topology at the center and the sheet evolves into three minima of the absolute magnetic field at (x,y) = (−2.4,2.5) cm, (1,−1.9) cm, and (2.7,−5.1) cm (II). As the reconnecting magnetic field approaches zero, the only contribution comes from the extracted current, and the resulting topology is an O-point (III). As the drive current reverses direction the three null points are again formed at (x,y) = (−4.5,−5) cm, (0.9,1.4) cm, and (6,2.3) cm, but in the push reconnection phase (IV). When no current is flowing, the X-point and the minimum of the absolute magnetic field is located at (x,y) = (0,0) cm, but as a result of the gun not being placed precisely at the X-point it gets shifted by the gun current. This shift can be seen in all plots of the magnetic field (b)–(e) and it is also the reason for the asymmetry of the three minima in Figure 5(c). From Figures 5(f)–5(i) it can be seen that the extracted current maximum is at (x,y) = (0.9,−1.3) cm. It is also clear that the in-plane magnetic field barely modifies the shape of the current sheet. The position and shape of sheet is mainly determined by the position and aperture of the plasma gun. This is due to the guide field being much higher in comparison to the in-plane reconnection field for the latter to be able to significantly influence the shape.

Reconnection measurements using setup B are shown in Figure 6. Figure 6(a) shows again the oscillating current through the third conductor (solid line), the current extracted from the plasma gun (dashed-dotted line), and the inductive electric field as approximated by time-derivative of the drive current (dotted line). The current through the parallel conductors creating the X-point topology was approximately 1 kA. Since the inductive field is much lower than for setup A (maximum of approximately 17 V/m at center), the current extracted from the gun is, as expected, also lower with a peak value of 9 A. Furthermore, the inductive field is not high enough to completely inhibit the background current but merely acts to modulate it. The absolute magnetic field and current density are plotted for three time points, indicated by roman numerals I–III in Figure 6(a). The motion of a field line is highlighted in 6(b)–6(d) with a dotted line. At time instant I the plasma gun discharge has not yet started and there is no current flowing (cf. Figure 6(e)). Hence, the field topology is defined by the two parallel conductors only. The field line remains stationary at this position until the gun starts discharging and the background current initially pushes the field line outwards. As the drive sets in, the field line is pushed further outwards until the current though the conductors reaches its maximum and the inductive field changes direction (time instant II). At this point in time, the current in Figure 6(f)

mainly consists of the background current. The inductive field then starts to extract an additional current as the field line starts to be pulled back. At time instant IV, the extracted current has reached its maximum of 9 A. In Figure 6(f), the current density can clearly be seen to have increased due to the inductive field. Shortly afterwards, the drive current reaches its maximum and the inductive field changes direction again, and as a result the field line is once more pushed away. From Figures 6(b)–6(e), it is clear that the neutral sheet remains throughout the reconnection event and does not evolve into three minima as in the case of setup A. This is due to the current being much lower and not as highly concentrated at the X-point. The X-point is also initially at (x,y) = (0,0) cm but can be seen to move slightly due to the asymmetry of the third coil, to (x,y) = (0,0.5) cm at time instant II and to (x,y) = (−1,0.5) cm at time instant III, but the motion is much smaller than the current sheet width.

Since this measurement was made using a much smaller guide field than in the measurement with setup A, the current sheet is no longer determined solely by the aperture of the plasma gun but is instead modified by the X-point topology and elongated along the separatrix.

IV. SUMMARY AND CONCLUSION

A new experiment, VINETA II, dedicated to the study of driven magnetic reconnection was presented. The main research goals of the device are to study the fluctuations associated with reconnection, the effect of boundary conditions, three-dimensional reconnection, and the influence of the guide field. The setup of the experiment is highly versatile and allows for a number of important parameters influencing the reconnection event to be changed independently. The range of plasma parameters achievable in the device, along with the timescale of the drive, also allows for the study of reconnection in both collisional and near collisionless reconnection.

The driving of the field lines is achieved either by an oscillating current through two parallel conductors (setup A), or by having a stationary X-point topology and driving the reconnection by an oscillating current through a third conductor (setup B). For setup A, the current drawn from the gun was found to dominate the magnetic field topology at the X-point, tearing the neutral sheet apart and forming three minima. This result was similar to what Stenzel and Gekelmann[28] found in their experiment at UCLA.[12] There are also periods of time when an inductively driven current is flowing but no X-point topology is present. Furthermore, the driving of the flux is done by the same coils generating it, which complicates the interpretation of the data. Setup B was found to be a more suitable approach to drive the reconnection since the inductive field can be set independently of the X-point topology and hence the current can be varied. Additionally, the X-point topology is always present and the flux is simply moved in and out of the X-point. However, due to the asymmetry introduced by the third coil, the X-point moves slightly due to the oscillating current. If needed this could be circumvented by using four conductors instead of three. It was found that the shape of the current sheet was mainly determined by the aperture of the gun for high B_{guide}/B_{rec}. A planned upgrade of the PFN will allow for an increase of the in-plane field, and hence for the X-point topology to have a significant effect on the current sheet geometry also at high B_{guide}.

[1] D. Biskamp, *Magnetic Reconnection in Plasmas* (Cambridge University Press, 2000).
[2] M. Yamada, R. Kulsrud, and H. Ji, Rev. Mod. Phys. **82**, 603 (2010).
[3] A. Bhattacharjee, Annu. Rev. Astron. Astrophys. **42**, 365 (2004).
[4] E. N. Parker, J. Geophys. Res. **62**, 509, doi:10.1029/JZ062i004p00509 (1957).
[5] C. T. Russell, Geophys. Monogr. Ser. **30**, 124 (1984).
[6] B. Kadomtsev, Sov. J. Plasma Phys. **1**, 389 (1975).
[7] J. Wesson, *Tokamaks* (Clarendon, Oxford, 1987).
[8] J. Egedal, M. Øieroset, W. Fox, and R. Lin, J. Geophys. Res. **107**, 1230, doi:10.1029/2001JA000287 (2002).
[9] M. Øieroset, T. Phan, M. Fujimoto, R. Lin, and R. Lepping, Nature (London) **412**, 414 (2001).
[10] W. Daughton, V. Roytershteyn, H. Karimabadi, L. Yin, B. Albright, B. Bergen, and K. Bowers, Nature Phys. **7**, 539 (2011).
[11] A. Zeiler, D. Biskamp, J. F. Drake, B. N. Rogers, M. A. Shay, and M. Scholer, Phys. Rev. Lett. **94**, 025006 (2005).
[12] T. Tharp, M. Yamada, H. Ji, E. Lawrence, S. Dorfman, C. E. Myers, and J. Yoo, Phys. Rev. Lett. **109**, 165002 (2012).
[13] Y. Ono, A. Morita, M. Katsurai, and M. Yamada, Phys. Fluids **5**, 3691 (1993).
[14] M. Yamada, Y. Ren, H. Ji, J. Breslau, S. Gerhardt, R. Kulsrud, and A. Kuritsyn, Phys. Plasmas **4**, 1936 (1997).
[15] J. Egedal, A. Fasoli, M. Porkolab, and D. Tarkowski, Rev. Sci. Instrum. **71**, 3351 (2000).
[16] A. Frank, Phys. Plasmas **12**, 052316 (2005).
[17] M. R. Brown, Phys. Plasmas **6**, 1717 (1999).
[18] I. Furno, T. Intrator, E. Torbert, C. Carey, M. Cash, J. Campbell, W. Fienup, C. Werley, G. Wurden, and G. Fiksel, Rev. Sci. Instrum. **74**, 2324 (2003).
[19] C. Paz-Soldan, W. F. Bergerson, M. I. Brookhart, D. A. Hannum, R. Kendrick, G. Fiksel, and C. B. Forest, Rev. Sci. Instrum **81**, 123503 (2010).
[20] H. Ji, M. Yamada, S. Hsu, and R. Kulsrud, Phys. Rev. Lett. **80**, 3256 (1998).
[21] H. Ji, M. Yamada, S. Hsu, R. Kulsrud, T. Carter, and S. Zaharia, Phys. Plasmas **6**, 1743 (1999).
[22] M. Yamada, Y. Ren, H. Ji, J. Breslau, S. Gerhardt, R. Kulsrud, and A. Kuritsyn, Phys. Plasmas **13**, 052119 (2006).
[23] M. Fujimoto, I. Shinohara, and H. Kojima, Space Sci. Rev. **160**, 123 (2011).
[24] S. Masuda, T. Kosugi, H. Hara, S. Tsuneta, and Y. Ogawara, Nature (London) **371**, 495 (1994).
[25] M. Kivelson and C. Russell, *Introduction to Space Physics* (Cambridge University Press, 1995).
[26] A. H. Boozer, Phys. Plasmas **19**, 112901 (2012).
[27] M. Yamada, H. Ji, S. Hsu, T. Carter, R. Kulsrud, Y. Ono, and F. Perkins, Phys. Rev. Lett. **78**, 3117 (1997).
[28] W. Gekelman, R. Stenzel, and N. Wild, J. Geophys. Res. **87**, 101, doi:10.1029/JA087iA01p00101 (1982).
[29] E. Zweibel and M. Yamada, Annu. Rev. Astron. Astrophys. **47**, 291 (2009).
[30] C. Franck, O. Grulke, and T. Klinger, Phys. Plasmas **9**, 3254 (2002).
[31] C. Franck, O. Grulke, and T. Klinger, Phys. Plasmas **10**, 323 (2003).
[32] T. Windisch, K. Rahbarnia, O. Grulke, and T. Klinger, Plasma Sources Sci. Technol. **19**, 055002 (2010).
[33] P. Stangeby, *The Plasma Boundary of Magnetic Fusion Devices* (Institute of Physics Publishing, 2000).
[34] G. Fiksel, A. Almagri, D. Craig, M. Iida, S. Prager, and J. Sarff, Plasma Sources Sci. Technol. **5**, 78 (1996).
[35] H. White, P. Gillette, and J. Lebacqz, *Pulse Generators*, 1st ed. (McGraw-Hill, New York, 1948), Chap. 6, pp. 175–224.
[36] H. Ji and W. Daughton, Phys. Plasmas **18**, 111207 (2011).
[37] I. Hutchinson, *Principles of Plasma Diagnostics* (Cambridge University Press, 1987).
[38] C. Franck, O. Grulke, and T. Klinger, Rev. Sci. Instrum. **73**, 3768 (2002).